

Articles

Reaction of Pyrones with Triosmium Clusters

Qi Lin and Weng Kee Leong*

Department of Chemistry, National University of Singapore, Kent Ridge, Singapore 119260

Received April 4, 2003

Reaction of $\text{Os}_3(\text{CO})_{10}(\text{NCCH}_3)_2$, **2**, with coumarin, chromone, α -pyrone, γ -pyrone, or 2-methyl-3-hydroxy- γ -pyrone afforded the products $\text{Os}_3(\text{CO})_{10}(\mu\text{-H})(\mu\text{-L})$, **3**, in which the pyrone is anchored onto the triosmium framework via the exocyclic oxygen and orthometalation; the major product for the last pyrone is $\text{Os}_3(\text{CO})_9(\mu\text{-H})(\mu\text{-}\gamma\text{-C}_6\text{H}_5\text{O}_3)$, **5**, coordinated via the hydroxyl group rather than an orthometalation. The cluster $\text{Os}_3(\text{CO})_{10}(\mu\text{-H})(\mu\text{-OH})$, **7**, formed H-bonded adducts, **8**, with unsubstituted pyrones; the OH functioned as the H-donor.

Introduction

One current impetus in organometallic cluster chemistry has been the hope that the multinuclear cluster core may imbue unusual reactivity to a cluster-bound organic substrate. Indeed, this has been very elegantly demonstrated in the quinoline system by the group of Rosenberg.¹ It is thus of interest to examine the chemistry of cluster-bound organic substrates. A prerequisite for such studies is the anchoring of the organic substrate onto a cluster. Much effort has been expended on investigating the interaction of N-heterocycles with triosmium clusters. Thus osmium clusters containing ligands from the quinoline, pyridine, pyrazole, imidazole, and pyrrole families are known.² In contrast, there are very few osmium clusters known that contain O-heterocycles.³

* Corresponding author.

(1) (a) Joynal, A. M.; Bergman, B.; Holmquist, R.; Smith, R.; Rosenberg, E.; Ciurash, J.; Hardcastle, K.; Roe, J.; Vazquez, V.; Roe, C.; Kabir, S.; Roy, B.; Alam, S. and Azam, K. A. *Coord. Chem. Rev.* **1999**, *190–192*, 975. (b) Kabir, S. E.; Kolwaite, D. S.; Rosenberg, E.; Hardcastle, K. I.; Cresswell, W. and Grindstaff, J. *Organometallics* **1995**, *14*, 3611. (c) Abedin, M. J.; Bergman, B.; Holmquist, R.; Smith, R.; Rosenberg, E.; Ciurash, J.; Hardcastle, K.; Roe, J.; Vazquez, V.; Roe, C.; Kabir, S. E.; Roy, B.; Alam, S. and Azam, K. A. *Coord. Chem. Rev.* **1999**, *192*, 975. (d) Bergman, B.; Holmquist, R.; Smith, R.; Rosenberg, E.; Ciurash, J.; Hardcastle, K. I.; Visi, M. *J. Am. Chem. Soc.* **1998**, *120*, 12818.

(2) See for example: (a) Shapley, J. R.; Samkoff, D. E.; Bueno, C.; Churchill, M. R. *Inorg. Chem.* **1982**, *21*, 634. (b) Yin, C. C.; Deeming, A. J. *J. Chem. Soc., Dalton Trans.* **1975**, 2091. (c) Burgess, K.; Johnson, B. F. G.; Lewis, J. J. *Organomet. Chem.* **1982**, *233*, C55. (d) Deeming, A. J.; Peters, R.; Hursthouse, M. B.; Backer-Dirks, J. D. J. *J. Chem. Soc., Dalton Trans.* **1982**, 787. (e) Yin, C. C.; Deeming, A. J. *J. Chem. Soc., Dalton Trans.* **1982**, 2563. (f) Deeming, A. J.; Whittaker, C.; Arce, A. J.; De Sanctis, Y. *J. Organomet. Chem.* **1997**, *540*, 67. (g) Leadbeater, N. E.; Lewis, J.; Raithby, P. R.; Ward, G. P. *Eur. J. Inorg. Chem.* **1998**, 1479. (h) Day, M. W.; Hardcastle, K. I.; Deeming, A. J.; Arce, A. J.; De Sanctis, Y. *Organometallics* **1990**, *9*, 6. (i) Chao, M.-H.; Kumaresan, S.; Wen, Y.-S.; Lin, S.-C.; Hwu, J. R.; Lu, K.-L. *Organometallics* **2000**, *19*, 714.

(3) (a) Azam, K. A.; Deeming, A. J.; Kimber, R. E.; Shukla, P. R. *J. Chem. Soc., Dalton Trans.* **1976**, 1853. (b) Arce, A. J.; De Sanctis, Y.; Deeming, A. J. *J. Organomet. Chem.* **1986**, *311*, 371. (c) Boyer, E.; Deeming, A. J.; Randle, N. P.; Bates, P. B.; Hursthouse, M. B. *J. Chem. Soc., Dalton Trans.* **1987**, 551. (d) Tunik, S. P.; Balova, I. A.; Borovitev, M. E.; Nordlander, E.; Haukka, M.; Pakkanen, T. A. *J. Chem. Soc., Dalton Trans.* **2002**, 827.

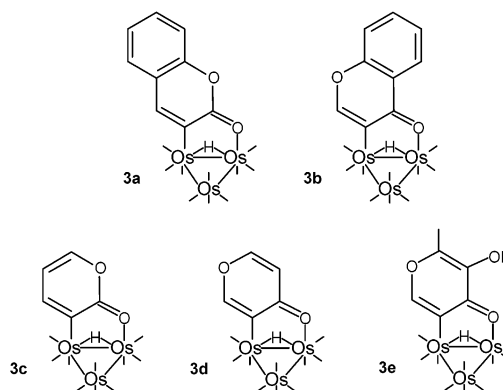


Figure 1. Molecular structures of clusters **3**.

The pyrones are an important class of O-heterocycles that occur in many naturally occurring compounds such as several steroids and kojic acid and in important drugs such as the anticoagulant warfarin. The α - and γ -pyrone ring systems possess little aromaticity, the former behaving more like an unsaturated lactone and the latter a vinylogous lactone. It is possible, however, to aromatize them via electrophilic attack at the exocyclic oxygen.⁴ In this paper, we would like to report our investigations into the reaction of two triosmium clusters, namely, $\text{Os}_3(\text{CO})_{10}(\text{CH}_3\text{CN})_2$, **2**, and $\text{Os}_3(\text{CO})_{10}(\mu\text{-H})(\mu\text{-OH})$, **7**, with a number of representative pyrones in order to map out their behavior with organometallic clusters, particularly in relation to their binding onto the cluster.

Results and Discussion

The reaction of **2** with excess coumarin, chromone, α -pyrone, γ -pyrone, or 2-methyl-3-hydroxy- γ -pyrone at elevated temperatures afforded products with the molecular formula $\text{Os}_3(\text{CO})_{10}(\mu\text{-H})(\mu\text{-L})$, **3** (L = $\alpha\text{-C}_9\text{H}_5\text{O}_2$ (**a**); $\gamma\text{-C}_9\text{H}_5\text{O}_2$ (**b**); $\alpha\text{-C}_5\text{H}_3\text{O}_2$ (**c**); $\gamma\text{-C}_5\text{H}_3\text{O}_2$ (**d**); 2-Me-3-OH- $\gamma\text{-C}_5\text{HO}_2$ (**e**)), as illustrated below (Figure 1).

(4) Gilchrist, T. L. *Heterocyclic Chemistry*, 3rd ed.; Longman: Singapore, 1997.

Table 1. Spectroscopic and Analytical Data for All Products

cluster	IR [$\nu(\text{CO})/\text{cm}^{-1}$]	$^1\text{H NMR}$ [$\delta/(\text{ppm})$] ^a	$J_{\text{H-H}}$ [Hz]	MS [m/z]	Anal. (calcd)	
					C	H
3a	2106w, 2068s, 2054s, 2024s, 2012w(sh), 2006s, 1996m, 1988w (sh), 1977w	8.44(s, H ₄), 7.6–7.2(4H, m, benzo), –12.8(s, OsHOs) ^a			23.13 (22.89)	0.39 (0.61)
3b	2105w, 2066s, 2053s, 2036w, 2022s, 2007s, 1993m, 1986w(sh), 1975w	8.18(s, H ₂), 7.94(d, H ₅), 7.67 (m, H ₇), 7.49(d, H ₈), 7.42(m, H ₆), –12.8(s, OsHOs) ^b	$^3J_{56} = ^3J_{78} = 8.2$, $^4J_{57} = ^4J_{68} = 1.6$	-	22.86 (22.89)	0.44 (0.61)
3c	2106w, 2068s, 2054s, 2024s, 2012w(sh), 2006s, 1996m, 1987w(sh), 1977w	8.06(dd, H ₆), 7.42(dd, H ₄), 6.30(dd, H ₅), –13.1(s, OsHOs)	$^3J_{45} = 4.9$, $^4J_{46} = 1.6$, $^3J_{56} = 6.6$	947.6 ^d 945.7 ^e	18.88 (19.03)	0.31 (0.43)
3d	2106w, 2066s, 2053s, 2023s, 2006s, 1994m, 1987w(sh), 1975w	7.99(s, H ₂), 7.66(d, H ₆), 6.33 (d, H ₅), –13.0(s, OsHOs)	$^3J_{56} = 5.0$		19.11 (19.03)	0.64 (0.43)
3e	2106w, 2066s, 2054s, 2023s, 2007s, 1994m, 1987w(sh), 1976w	7.84(s, H ₆), 5.51(s, OH), 2.39 (3H, s, Me), –12.9(s, OsHOs)			19.33 (19.67)	0.70 (0.62)
4	2112w, 2077s, 2060s, 2030s, 2014s, 2005m(sh), 1993w, 1985w	6.85(dd, H ₄), 6.11(d, H ₅), 5.71 (d, H ₃), –13.6(s, OsHOs)	$^3J_{34} = 9.1$, $^3J_{45} = 6.6$	947.7 ^d 944.6 ^e	f	f
5	2102w, 2059s, 2022m(sh), 2019vs, 2003s, 1987w, 1982vw(sh), 1941w	7.78(d, H ₆), 6.73(d, H ₅), 2.46 (s, 3H, Me), –9.3(s, OsHOs)	$^3J_{56} = 5.0$		19.24 (18.99)	0.46 (0.64)
6	2126w, 2082vw, 2069m, 2049s, 2022m, 2008m, 1994w, 1983w, 1937w	8.09(d, H ₅), 7.84(d, H ₃), 7.74 (t, H ₇), 7.63(t, H ₂), 7.60(d, H ₈), 7.37(t, H ₆), 7.00(d, H ₁), –14.5 (s, OsHOs)	$^3J_{23} = ^3J_{67} = 7.4$, $^3J_{12} = ^3J_{56} = ^3J_{78} = 8.2$, $^4J_{57} = ^4J_{68} = 1.6$		f	f
8a	2108vw, 2067s, 2057m, 2019s, 1997m, 1990vw(sh), 1983w, 1978w(sh)	7.71(d, H ₄), 7.53(t, H ₇), 7.50 (d, H ₅), 7.31(d, H ₈), 7.27(t, H ₆), 6.37(d, H ₃), 0.42(s, OH), –12.64 (s, OsHOs) ^b	$^3J_{34} = 10$, $^3J_{56} = ^3J_{78} = 8.2$, $^4J_{57} = ^4J_{67} = 1.6$		22.54 (22.48)	0.45 (0.79)
8b	2109vw, 2068s, 2058m, 2021s, 2000m, 1989w(sh), 1983w	8.22(d, H ₅), 7.85(d, H ₂), 7.68 (m, H ₇), 7.46(d, H ₈), 7.41(m, H ₆), 6.34(d, H ₃), 0.52(s, OH), –12.62(s, OsHOs)	$^3J_{23} = 5.8$, $^3J_{56} = 8.2$, $^3J_{78} = 8.2$		22.31 (22.48)	0.49 (0.79)
8c	2109vw, 2068s, 2059m, 2022s, 2002m, 1990w(sh), 1984w, 1978w(sh)	8.36(2H, d, H ₁ & H ₈), 7.77 (2H, t, H ₃ & H ₆), 7.52(2H, d, H ₄ & H ₅), 7.39(2H, t, H ₂ & H ₇), 0.59(s, OH), –13.12(s, OsHOs) ^c	$^3J = 8.2$, $^4J = 1.6$		25.99 (25.94)	0.88 (0.95)
8d	2109vw, 2068s, 2058m, 2020s, 1990w, 1982w, 1978w(sh)	7.70(2H, d, H ₂ & H ₆), 6.31(2H, d, H ₃ & H ₅), 0.70(s, OH), –12.65 (s, OsHOs)	$^3J_{23} = ^3J_{56} = 6.2$		18.74 (18.67)	0.54 (0.63)
8e	2109vw, 2068s, 2058m, 2021s, 2015m(sh), 1999w, 1983w, 1978w(sh), 1761vs	6.44(d, H ₆), 6.12(ddd, H ₄), 5.71 (d, H ₃), 5.05(t, H ₅), 0.60(s, OH), ^c –13.09(s, OsHOs) ^c	$^3J_{34} = 9.6$, $^3J_{45} = ^3J_{56} = 5.2$, $^3J_{46} = 1.8$		18.71 (18.67)	0.42 (0.63)
9	2118m, 2089s, 2063vs, 2045w, 2029s, 2018m, 2003m, 1999m(sh), 1984vw	5.40(s, H ₃), 1.89(3H, s, Me), –11.9 (s, OsHOs), –14.1(s, OsHOs)			18.97 (18.99)	0.66 (0.64)
10	2102w, 2073vs, 2037s, 2016m, 2003m, 1968vw	5.61(s, H ₃), 1.90(3H, s, Me)			18.03 (17.70)	0.30 (0.33)

^a The integration is 1H unless otherwise indicated. ^b In CD₂Cl₂. ^c In *o*-toluene. ^d FAB-MS, M⁺. ^e FAB-MS, M⁻. ^f Unstable compound.

The clusters **3** have been characterized spectroscopically and analytically (Table 1), and for **3a–d**, by single-crystal X-ray crystallographic studies as well; the common atomic numbering scheme and selected bond parameters for clusters **3a–d** are given in Table 2.

The pyrones in the clusters **3** are bound to the cluster core via the exocyclic (ketonic) oxygen and an ortho-metalation; this is similar to that found in N-heterocycles^{1,2} and other O-heterocycles.³ In contrast to the benzo derivatives of those systems, however, we have not observed any product resulting from metalation of the benzo ring in coumarin or chromone. The pyrones are bound axially with respect to the triosmium plane; the dihedral angles between the Os₃ and the pyrone planes are about $97 \pm 1^\circ$. The bond parameters for the O-heterocycles in **3a–d** suggest that the bonding within the heterocycles is not much affected by coordination to the cluster.⁵ A noticeable structural feature common to all the clusters is the shortening of the Os–CO bond trans to the O donor atom; the sum of the Os–C and C–O bond lengths⁶ for this carbonyl is the shortest (except for **3b**, where the disorder of the chromone ring renders the associated bond parameters less reliable) and reflects the increase in π -back-donation into this carbonyl.

The $^1\text{H NMR}$ spectra of **3a–e** have been assigned by comparison with the resonances for the free pyrones.⁷ Thus in the $^1\text{H NMR}$ spectrum of **3b** (Figure 2) for

example, the absence of the H3 resonance at about δ 6.4 ppm compared to the spectrum of chromone indicates that metalation has occurred at C3. The singlet at δ 8.2 ppm is therefore assigned to H2; the assignments of the remaining resonances of **3b** are in accordance with those of free chromone.

It is thus observed that, on bonding to the clusters, the ^1H resonances of the pyrones are shifted downfield. In particular, that for the proton on the carbon atom adjacent to the metalated site exhibits a very large downfield shift (>0.3 ppm). This suggests that the aromaticity of the pyrone rings is increased slightly and that the non-carbonyl carbon adjacent to the metalation site is relatively electron-deficient. Interestingly, the hydroxyl resonance in **3e** is narrow (width < 0.2 ppm), unlike the very broad signal (width > 3 ppm) in the free pyrone, and suggests that exchange of the hydroxyl H with adventitious water is inhibited on attachment of the pyrone onto the cluster.

In the reaction of α -pyrone, another product, **4**, was also isolated. This product is thermally unstable; attempts at crystallization at low temperature afforded only **3c** and other unidentified decomposition products.

(5) Allen, F. H.; Kennard, O.; Watson, D. G.; Brammer, L.; Orpen, A. G.; Taylor, R. *J. Chem. Soc., Perkin Trans.* **1987**, S1.

(6) Leong, W. K.; Einstein, F. W. B.; Pomeroy, R. K. *J. Cluster Sci.* **1996**, 7, 121.

(7) *Handbook of Proton-NMR Spectra and Data*; Asahi Research Center Co., Ltd., Ed.; Academic Press Inc: Japan, 1986.

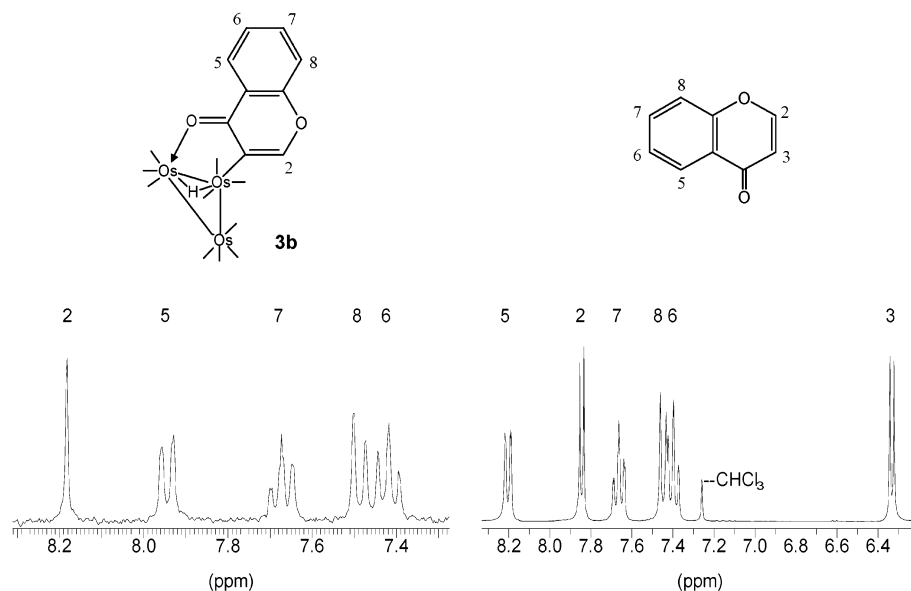


Figure 2. ^1H NMR spectra and tentative assignments for **3b** (left) and chromone (right).

Table 2. Common Atomic Numbering Scheme and Selected Bond Parameters for Clusters 3a–d

	3a	3b ^a	3c	3d
Bond Lengths (Å)				
Os(1)Os(2)	2.9327(4)	2.9089(6)	2.9321(17)	2.9062(4)
Os(2)Os(3)	2.8990(4)	2.8925(6)	2.9414(15)	2.9136(4)
Os(3)Os(1)	2.8750(4)	2.8977(6)	2.9092(14)	2.8884(4)
Os(1)O(1)	2.135(5)	2.16(2)	2.135(10)	2.127(5)
Os(2)C(2)	2.159(7)	2.14(3)	2.150(14)	2.146(7)
O(1)C(1)	1.226(9)	1.38(2)	1.260(17)	1.263(9)
C(1)C(2)	1.464(10)	1.35(3)	1.460(19)	1.443(12)
C(2)C(3)	1.365(10)	1.40(3)	1.39(2)	1.368(11)
C(3)C(4)/C(3)O(4)	1.446(10)	1.39(2)	1.41(2)	1.360(10)
C(4)C(5)/O(4)C(5)	1.390(10)	1.260(15)	1.32(3)	1.324(13)
C(5)O(6)/C(5)C(6)	1.378(9)	1.394(14)	1.38(2)	1.336(14)
O(6)C(1)/C(6)C(1)	1.357(9)	1.460(13)	1.373(16)	1.434(10)
Bond Angles (deg)				
Os(2)Os(1)Os(3)	59.880(10)	59.754(14)	60.47(4)	60.370(10)
Os(1)Os(2)Os(3)	59.073(10)	59.931(14)	59.38(2)	59.513(9)
Os(1)Os(3)Os(2)	61.047(10)	60.314(14)	60.15(4)	60.117(10)
O(1)Os(1)Os(2)	82.75(14)	83.3(6)	83.0(3)	83.66(16)
C(2)Os(2)Os(1)	82.68(19)	83.7(9)	83.2(4)	82.5(2)
Dihedral angle between Os(1)Os(2)Os(3) and Os(1)O(1)C(1)C(2)Os(2)	97.7(2)	96.9(9)	97.4(4)	96.0(2)

^a Disorder of chromone.

Consistent with this was the observation that the relative amounts of **3c** and **4** obtained depended on the reaction temperature employed. Thus in refluxing hexane, they were obtained in about equal amounts, whereas in refluxing toluene, the amount of **4** obtained was negligible.

The IR spectrum of **4** in the carbonyl stretch region is very similar to that of the clusters **3**, suggesting similar number and arrangement of carbonyl ligands in the two; this is also supported by the FAB-MS, which showed a cluster of peaks centered at m/z 947.7, corresponding to M^+ .

A comparison of the ^1H NMR spectrum of **4** with that of α -pyrone (Figure 3) suggests that C6 has been metalated. This would also imply that, in contrast to the clusters **3**, the ^1H resonances for the pyrone in **4** are shifted upfield; that for H3 is particularly large. This would be consistent with a loss of aromaticity on bonding at the endocyclic oxygen, which is expected to reduce the aromatic canonical form of α -pyrone.

Similarly, the major product from the reaction of 2-methyl-3-hydroxy- γ -pyrone was a second product, $\text{Os}_3(\text{CO})_9(\mu\text{-H})(\mu\text{-}\gamma\text{-C}_6\text{H}_5\text{O}_3)$, **5**. The molecular structure of **5** has been determined by a single-crystal X-ray crystallographic study, and the ORTEP diagram is shown in Figure 4, together with selected bond parameters. Unlike in **3e**, cluster **5** has the hydroxyl group involved in coordination to the cluster, rather than an orthometalation. The bond parameters associated with the pyrone again suggest that the effect on the pyrone on binding to the cluster is small. The higher yield of **5** compared to **3e** suggests that the cleavage of the O–H bond in the hydroxyl group of 2-methyl-3-hydroxy- γ -pyrone is more favored than orthometalation, as may be expected.

That the pyrones appear to favor metalation at the ortho position to the exocyclic oxygen prompted us to examine the case with xanthone, in which it is not possible for orthometalation to the exocyclic oxygen to occur. The reaction afforded one major product, **6**. Monitoring by IR spectroscopy showed that **6** decomposed slowly to afford $\text{Os}_3(\text{CO})_{12}$, **1**. The ^1H NMR spectrum of **6** (Figure 5) showed seven sets of non-equivalent resonances, indicating metalation of the xanthone has occurred; none of these were singlets, thus pointing to C1, C4, C5, or C8 as the possible metalation sites. The benzo resonances H5 to H8 may be assigned by comparison with that in free xanthone, leaving the resonances for the metalated ring, which are shifted upfield with respect to the benzo resonances. This suggests that the endocyclic oxygen is bonded to the clusters, just as in **4**; the tentative structure for **6** is given in the inset to Figure 5.

The cluster $\text{Os}_3(\text{CO})_{10}(\mu\text{-H})(\mu\text{-OH})$, **7**, has recently

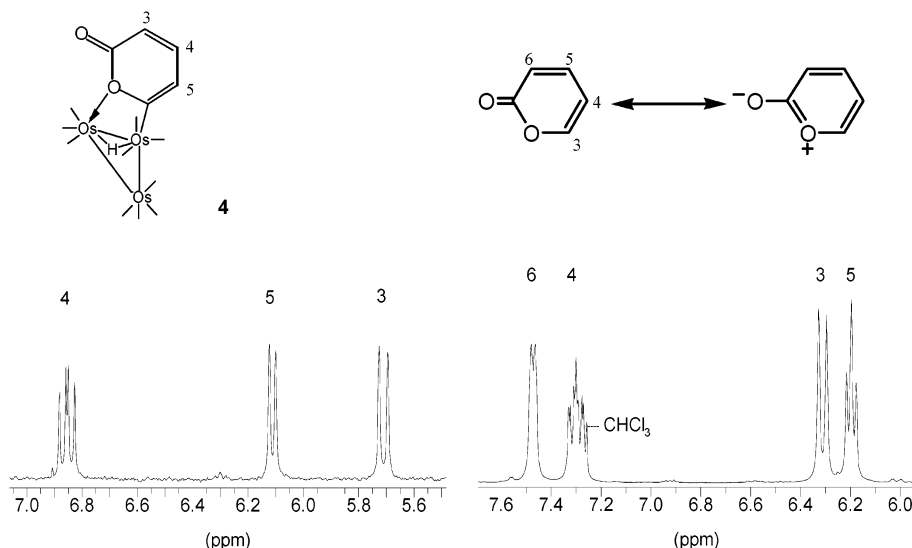


Figure 3. ^1H NMR spectra and tentative assignments for **4** (left) and α -pyrone (right).

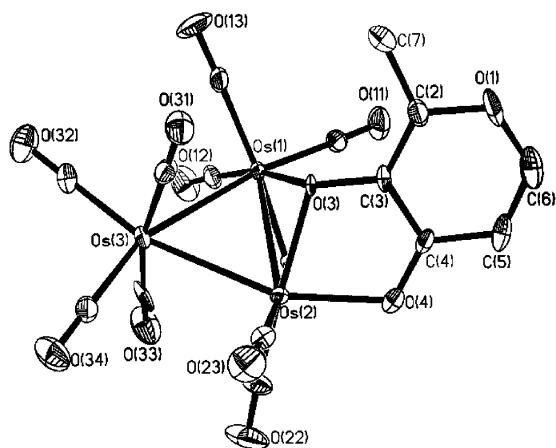


Figure 4. ORTEP diagram (50% probability thermal ellipsoids, organic hydrogens omitted) and selected lengths (Å) and angles (deg) for **5**. Os(1)Os(2) = 2.8000(4); Os(1)Os(3) = 2.8180(4); Os(2)Os(3) = 2.7642(4); Os(1)O(3) = 2.185(5); Os(2)O(3) = 2.142(5); Os(2)O(4) = 2.164(5); Os(3)C(31) = 1.937(7); O(1)C(6) = 1.350(11); O(1)C(2) = 1.353(9); C(2)C(3) = 1.355(10); C(2)C(7) = 1.483(11); C(3)O(3) = 1.364(8); C(3)C(4) = 1.421(10); C(4)O(4) = 1.276(9); C(4)C(5) = 1.417(10); C(5)C(6) = 1.321(13); Os(2)Os(1)Os(3) = 58.948(9); Os(3)Os(2)Os(1) = 60.851(9); Os(2)O(3)Os(1) = 80.62(16); C(3)O(3)Os(2) = 111.3(4); C(4)O(4)Os(2) = 112.8(4).

emerged as another useful precursor for tris-osmium cluster synthesis.^{8,13} The reaction of **7** with coumarin, chromone, xanthone, γ -pyrone, or α -pyrone afforded the H-bonded adducts, **8a–e**. These were characterized spectroscopically and analytically (Table 1), and for **8a** and **8d**, also by single-crystal X-ray crystallographic studies; the ORTEP diagram and selected bond lengths and bond angles for **8a** are given in Figure 6.

(8) Lum, M. W.; Leong, W. K. *J. Chem. Soc., Dalton Trans.* **2001**, 2476.

(9) Braga, D.; Grepioni, F. *Advances in Molecular Structure Research*; JAI: Greenwich, 1995; Vol. 2, p 25.

(10) Azam, K. A.; Deeming, A. J.; Rothwell, I. P.; Hursthouse, M. B.; New, L. J. *J. Chem. Soc., Chem. Commun.* **1978**, 1086.

(11) (a) Lu, C. Y.; Einstein, F. W. B.; Johnston, V. J.; Pomeroy, R. K. *Inorg. Chem.* **1989**, *28*, 4212. (b) Martin, L. R.; Einstein, F. W. B.; Pomeroy, R. K. *Inorg. Chem.* **1988**, *27*, 2986.

(12) Nicholl, J. N.; Vargas, M. D. *Inorg. Synth.* **1989**, *28*, 232.

(13) Roberto, D.; Lucenti, E.; Roveda, C.; Ugo, R. *Organometallics* **1997**, *16*, 5974.

The reactions were quantitative, as judged by IR spectroscopy. These H-bonded adducts are surprisingly thermally quite stable. For instance, the decomposition of **8a** in hexane became significant only when heated in a Carius tube above 100 °C, whereupon cluster decomposition occurred to afford $\text{Os}_3(\mu\text{-H})_2(\text{CO})_{10}$ (identified spectroscopically). On the other hand, they are completely transformed back to **7** during attempts at TLC separation on silica.

The formation of such O–H...O hydrogen bonds is novel; they are the first examples of a bridging OH group directly coordinated to a cluster core participating as H-donors, in contrast to the more common examples involving cluster-bound organic ligands with free hydroxyl functions.⁹ Preliminary investigations suggest that the H-bonding also occurs with other ketones such as benzophenone. The ^1H resonance at 0.35 ppm for the OH group in cluster **7** is, for those cases in which it is observable, shifted downfield in **8**; this resonance for cluster **7** has been verified by the disappearance of the signal upon the addition of D_2O , which also confirms that this hydrogen is very labile. The capability of the bridging OH group to form an H-bond implies that it is acidic, and in that sense, cluster **7** behaves as an alcohol.

The reaction of **7** with hydroxyl-substituted pyrones followed a very different course. Thus the reaction between **7** and excess 2-methyl-3-hydroxy- γ -pyrone at temperatures from 25 to 60 °C gave rise to the partial formation of a complex that has an IR spectrum similar to that of **8a**. However, the complex could not be separated from **7** despite several attempts at recrystallization. Instead, cluster **5** was obtained as the major product when the mixture was further heated at 110 °C for 16 h. Presumably, the reaction at higher temperature is primarily driven by the hydroxy substituent on the pyrone; this is consistent with the behavior of **7** toward simple alcohols.^{8,13}

The reaction between **7** and 6-methyl-4-hydroxy- α -pyrone at 60 °C afforded the novel cluster $\text{Os}_3(\text{CO})_9(\mu\text{-H})_2(\mu_3\text{-}\alpha\text{-C}_6\text{H}_4\text{O}_3)$, **9**, in good yield. In refluxing toluene, another novel cluster, $\text{Os}_4(\text{CO})_{12}(\mu_4\text{-}\alpha\text{-C}_6\text{H}_4\text{O}_3)$, **10**, was obtained in 13% yield. It was also found that refluxing **9** in toluene gave **10**; the results are summarized in Scheme 1.

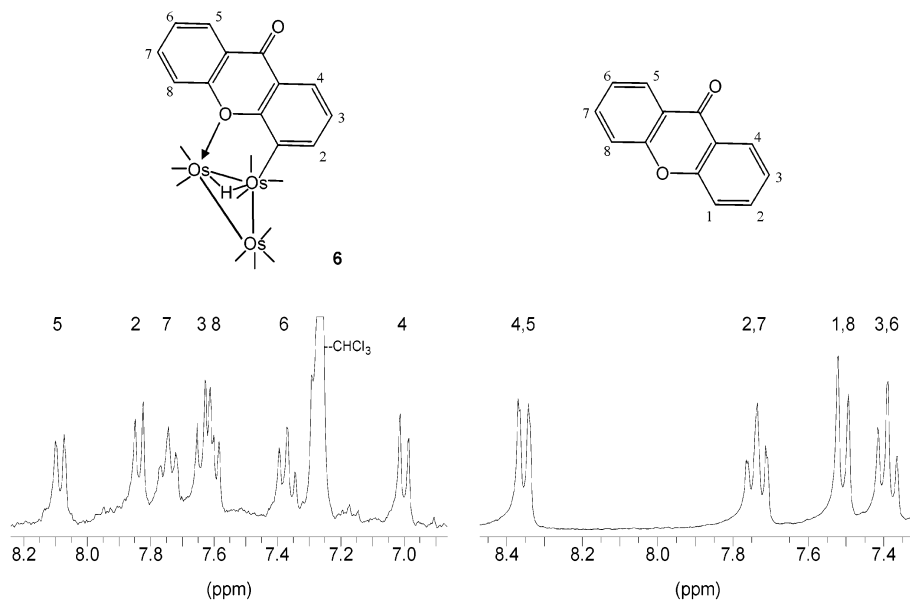


Figure 5. ^1H NMR spectra and tentative assignments for **6** (left) and xanthone (right).

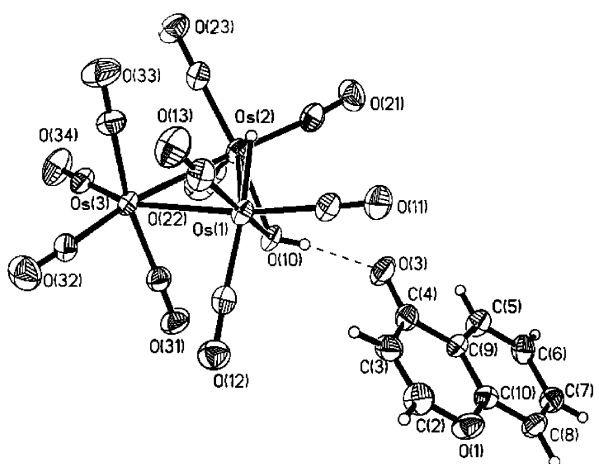


Figure 6. ORTEP diagram (50% probability thermal ellipsoids, organic hydrogens omitted) and selected lengths (Å) and angles (deg) for **8a**. Os(1)Os(2) = 2.7770(3); Os(1)Os(3) = 2.8195(3); Os(2)Os(3) = 2.8194(3); Os(1)O(10) = 2.102(5); Os(2)O(10) = 2.103(4); O(1)C(2) = 1.338(8); O(1)C(6) = 1.392(7); O(7)C(4) = 1.253(8); C(2)C(3) = 1.304(10); C(3)C(4) = 1.429(9); C(5)C(6) = 1.381(8); C(4)C(9) = 1.453(8); C(5)C(6) = 1.353(9); C(5)C(9) = 1.428(9); C(6)C(7) = 1.419(9); C(7)C(8) = 1.358(9); C(8)C(10) = 1.394(9); Os(2)Os(1)Os(3) = 60.494(8); Os(1)Os(2)Os(3) = 60.499(8); Os(2)Os(3)Os(1) = 59.006(8); O(10)Os(1)Os(3) = 80.13(13); O(10)Os(2)Os(1) = 48.66(12); Os(1)O(10)Os(2) = 82.65(16).

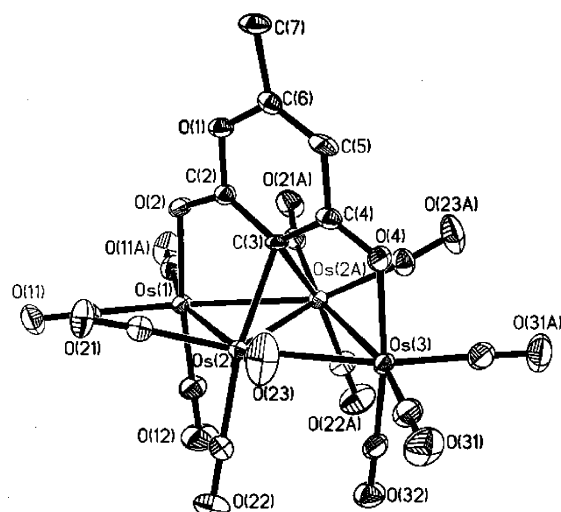


Figure 7. ORTEP diagram (50% probability thermal ellipsoids, organic hydrogens omitted) and selected lengths (Å) and angles (deg) for **8d**. Os(1)Os(2) = 2.7832(4); C(3)C(4) = 1.401(14); Os(1)Os(3) = 2.8196(4); C(9)C(10) = 1.373(9); Os(2)Os(3) = 2.8217(4); Os(1)O(10) = 2.114(5); Os(2)O(10) = 2.108(6); O(1)C(2) = 1.291(17); O(1)C(10) = 1.296(15); O(3)C(4) = 1.253(11); C(2)C(3) = 2.188(18); Os(2)Os(1)Os(3) = 60.475(9); O(10)Os(1)Os(3) = 80.03(16); Os(1)Os(2)Os(3) = 60.402(10); O(10)Os(2)Os(1) = 48.87(14); Os(2)Os(3)Os(1) = 59.123(9); Os(1)O(10)Os(2) = 82.5(2).

Clusters **9** and **10** were characterized completely, including by single-crystal X-ray crystallographic studies. The ORTEP diagrams are shown in Figures 8 and 9, respectively; selected bond lengths and bond angles are given in Table 3.

Cluster **9** is analogous to the known cluster $\text{Os}_3(\text{CO})_9(\mu\text{-H})_2(\mu_3\text{-C}_6\text{H}_4\text{O})$ obtained from the reaction of **1** with phenol, in which the phenol has lost its aromatic character.¹⁰ The C–C and C–O bond lengths of the pyrone in **9** are also consistent with this (depicted in Scheme 1); thus the C(4)–O(4) and C(5)–C(6) bond lengths of 1.268(10) and 1.309(13) Å, respectively, are indicative of double-bond character, while those of the others are consistent with single-bond character.

The tetraosmium cluster **10** has a rhombic arrangement of the osmium atoms. Few structural studies on tetraosmium clusters with such a planar arrangement of the osmium atoms have been reported, two examples being $\text{Os}_4(\mu\text{-H})(\text{CO})_{14}(\text{SnMe}_3)$ and $\text{Os}_4(\mu\text{-H})_2(\text{CO})_{13}(\text{PMe}_3)$.¹¹ The pyrone in **10** is coordinated to all four osmium atoms, and it is situated on one side of the tetraosmium plane. As in **9**, both the pyrone oxygen atoms are ketonic and the structure depicted in Scheme 1 is consistent with the observed bond parameters. As for the other clusters in this study, there is a discernible shortening of the Os–CO bond for the carbonyl trans to the O-donor.

Scheme 1

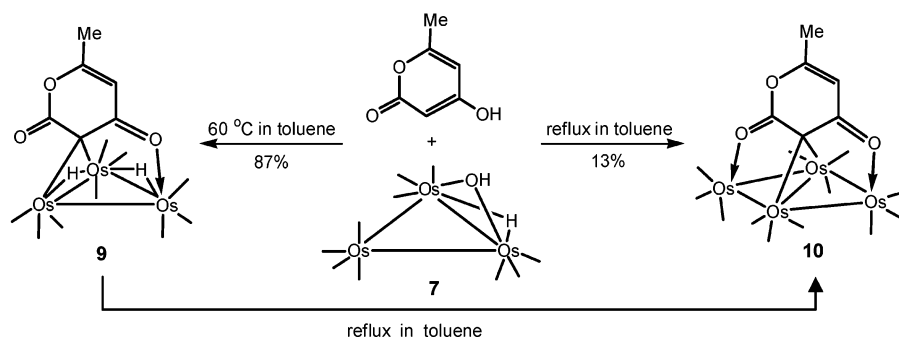
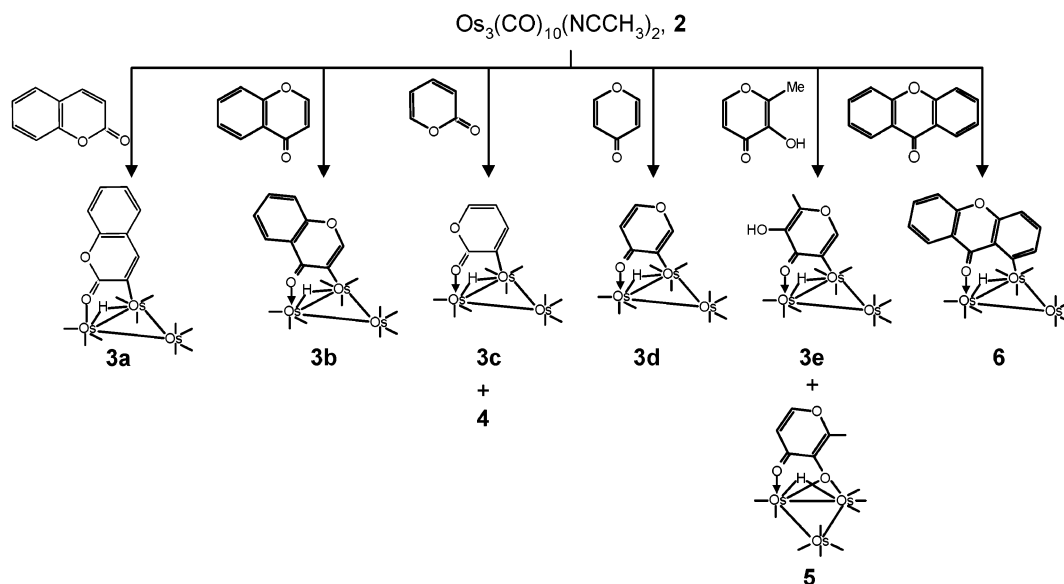


Table 3. Selected Bond Lengths (Å) and Bond Angles (deg) for 9 and 10

bond length	9	10	bond angle	9	10
Os(1)–Os(2) ^a	2.8063(4)	2.7039(4)	Os(2)–Os(1)–Os(3) ^a	57.716(12)	61.258(5)
Os(1)–Os(3) ^a	2.9464(5)	2.8075(3)	Os(3)–Os(2)–Os(1) ^a	63.672(13)	61.214(5)
Os(2)–Os(3)	2.7792(5)	2.8075(3)	Os(2)–Os(3)–Os(1) ^a	58.612(12)	57.572(10)
Os(1)–C(3) ^a	2.187(9)	2.204(5)	O(4)–Os(3)–Os(1) ^a	82.98(17)	84.21(13)
Os(2)–C(3)	2.193(9)	2.204(5)	O(4)–Os(3)–Os(2)	83.85(17)	84.21(13)
Os(3)–O(4)	2.105(6)	2.140(5)	C(3)–Os(1)–Os(3) ^a	73.5(2)	75.76(18)
O(1)–C(6)	1.379(12)	1.381(9)	C(3)–Os(2)–Os(3)	77.1(2)	75.76(18)
O(1)–C(2)	1.392(11)	1.363(9)	O(2)–C(2)–C(3)	126.2(8)	125.3(7)
O(2)–C(2)	1.206(12)	1.253(9)	Os(1)–C(3)–Os(2) ^a	79.7(3)	75.7(2)
O(4)–C(4)	1.268(10)	1.270(10)	O(4)–C(4)–C(3)	122.7(8)	122.2(7)
C(2)–C(3)	1.477(12)	1.420(10)	C(4)–O(4)–Os(3)	118.6(6)	118.0(5)
C(3)–C(4)	1.470(12)	1.436(10)	Os(2)–Os(1)–Os(2A)	N.A.	57.484(10)
C(4)–C(5)	1.416(12)	1.431(10)	Os(3)–Os(2)–Os(1)		121.844(9)
C(5)–C(6)	1.309(13)	1.334(12)	O(2)–Os(1)–Os(2)		83.68(12)
C(6)–C(7)	1.489(13)	1.490(10)	C(3)–Os(2)–Os(1)		76.31(18)
Os(1)–Os(2A)	N.A.	2.8063(4)			
Os(1)–Os(2)		2.8115(3)			
Os(1)–O(2)		2.157(5)			

^a For **10**, Os(1) is labeled as Os(2A).

Scheme 2



Concluding Remarks

The clusters **2** and **7** present different coordinative capabilities toward various pyrones. Cluster **2** interacts with pyrones via the ketone function and orthometallation, although the presence of a hydroxyl group tends to redirect the site of reaction. The reactions of **2** are summarized in Scheme 2.

Cluster **7** reacts with unsubstituted pyrones to form H-bonded adducts with its OH group functioning as the H-donor, while its reaction with hydroxyl-substituted

pyrones is favored by coordination via the hydroxyl function. Attachment of the pyrones onto the cluster core does not appear to significantly affect the structure of the pyrones. However, NMR evidence suggests enhanced aromaticity of the O-heterocycles in clusters **3**, implying that the coordinated pyrones will be more susceptible to electrophilic attack than the corresponding free pyrones. We have already embarked on investigating the chemistry of cluster-bound pyrones and will report some of our findings in a subsequent paper.

Table 4. Reaction Conditions and Yields for 2 with Coumarin, Chromone, Xanthone, or γ -Pyrone under Reflux

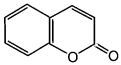
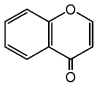
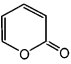
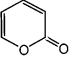
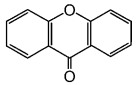
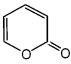
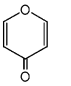
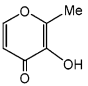
Amount of 2	Ligand	Amount of ligand	Solvent	Time (min)	Product	R_f	Yield
43.8 mg 0.047 mmol		34.4 mg 0.235 mmol	hexane	90	3a red crystals	0.56	22.2 mg (47%)
43.9 mg 0.047 mmol		34.0 mg 0.233 mmol	hexane	120	3b yellow crystals	0.58	15.0 mg (32%)
27.3 mg 0.029 mmol		1 drop	toluene	40	3c yellow crystals	0.46	3.9 mg (14%)
95.2 mg 0.102 mmol		4 drops	hexane	90	3c yellow crystals	0.46	9.3 mg (9.6%)
					4 yellow solid	0.29	10.0 mg (10%)
28.5 mg 0.031 mmol		12.0 mg 0.061 mmol	hexane	30	6 orange solid	0.44	2.2 mg (6.9%)

Table 5. Reaction Conditions and Yields for 2 with α -Pyrone, γ -Pyrone, or 2-Methyl-3-hydroxy- γ -pyrone in a Closed Vessel

Amount of 2	Ligand	Amount of ligand	Solvent	Temp. (°C)	Time (min)	Product	R_f	Yield
81.3 mg 0.087 mmol		8 drops	cyclohexane	110	40	3c yellow crystals	0.46	15.3 mg 19%
88.1 mg 0.094 mmol		8 drops	cyclohexane	110	40	3d yellow crystals	0.43	66.8 mg 75%
22.1 mg 0.094 mmol		23.7 mg 0.188 mmol	toluene	80	40	3e yellow solid	0.36	0.3 mg 1.3%
						5 yellow crystals	0.25	2.9 mg 13%

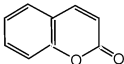
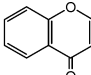
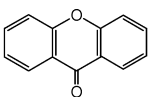
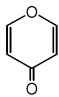
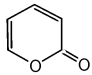
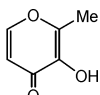
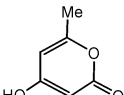
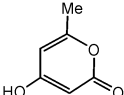
Experimental Section

General Procedures. All reactions and manipulations were carried out under nitrogen by using standard Schlenk techniques. Solvents were purified, dried, distilled, and stored under nitrogen prior to use. NMR spectra were recorded on a Bruker ACF-300 FT-NMR spectrometer as CDCl_3 solutions unless otherwise stated. ^1H chemical shifts reported are referenced against the residual proton signals of the solvents. ESI spectra were obtained on a Finnigan MAT LCQ, with a spray voltage of 4.5 kV and capillary temperature of 353 K, as CH_3CN solutions. FAB mass spectra were recorded on a Finnigan MAT 95XL-T mass spectrometer in a 3NBA matrix. EI spectra were obtained on a Macromass VG7035, at 70 eV. Microanalyses were carried out by the Microanalytical Laboratory at the National University of Singapore. The clusters

$\text{Os}_3(\text{CO})_{10}(\text{CH}_3\text{CN})_2$, **2**, and $\text{Os}_3(\text{CO})_{10}(\mu\text{-H})(\mu\text{-OH})$, **7**, were prepared according to literature methods.^{12,13} $\text{Os}_3(\text{CO})_{12}$, **1**, from OXKEM, and all other reagents from other commercial sources, were used as supplied. TLC separations were on plates coated with K60GF254 of 0.25 or 0.5 mm thickness, and extracted with dichloromethane.

Reactions of Pyrones with $\text{Os}_3(\text{CO})_{10}(\text{NCCH}_3)_2$, **2, under Reflux.** In a typical reaction, into a solution of **2** in hexane or toluene placed in a Schlenk tube fitted with a condenser was added an excess of the pyrone. The solution was refluxed under nitrogen, the solvent was then removed under reduced pressure, and the residue obtained was redissolved in the minimum volume of dichloromethane and chromatographed on TLC plates, hexane/ CH_2Cl_2 (4:1 v/v) as mobile phase. The reaction conditions and yields are summarized in Table 4.

Table 6. Reactions of 7 with Pyrones^a

Amount of 7	Ligand	Amount of ligand	Solvent	Temp./Time	Product	Yield
40.0 mg 0.046 mmol		33.7 mg 0.230 mmol	hexane	r. t. / 100 min	8a yellow crystals	*
40.0 mg 0.046 mmol		33.7 mg 0.230 mmol	hexane	r. t. / 100 min	8b yellow crystals	*
29.0 mg 0.033 mmol		19.7 mg 0.100 mmol	hexane	r. t. / 150 min	8c yellow crystals	*
12.1 mg 0.013 mmol		0.5 drop	hexane	40 °C / 4 h	8d yellow crystals	*
12.0 mg 0.013 mmol		0.5 drop	hexane	40 °C / 2 h	8e yellow crystals	*
39.4 mg 0.045 mmol		21.9 mg 0.174 mmol	toluene	reflux / 16 h	5 yellow crystals	27.5 mg 64%
19.8 mg 0.023 mmol		2.8 mg 0.023 mmol	toluene	60 °C / 18 h	9 light yellow crystals	18.9 mg 87%
72.0 mg 0.083 mmol		52.3 mg 0.416 mmol	toluene	reflux / 20 h	10 red crystals	12.3 mg 13%

^a * = quantitative reaction as judged from IR spectroscopy.

Reactions of Pyrones with Os₃(CO)₁₀(NCCH₃)₂, 2, in a Carius Tube. In a typical reaction, to a solution of **2** in cyclohexane or toluene in a Carius tube was added an excess of the pyrone. The solution was degassed by three freeze-pump-thaw cycles and heated for 40 min. The solvent was then removed under reduced pressure, and the residue obtained was redissolved in the minimum volume of dichloromethane and chromatographed. The reaction conditions and yields are summarized in Table 5.

Reactions of Pyrones with Os₃(CO)₁₀(μ-H)(μ-OH), 7. In a typical reaction, into a solution of **7** in hexane or toluene placed in a Schlenk tube fitted with a condenser was added an excess of the pyrone. The solution was stirred under nitrogen and monitored by IR spectroscopy. The solvent was then removed under reduced pressure, and the yellow solid residue was recrystallized from dichloromethane/hexane at -5 °C to afford yellow crystals of the product. For 2-methyl-3-

hydroxy-γ-pyrone and 6-methyl-4-hydroxy-α-pyrone, the residue obtained after solvent removal was redissolved in the minimum volume of dichloromethane and chromatographed on TLC plates with hexane/CH₂Cl₂ (3:2 v/v) as mobile phase. The reaction conditions and yields are summarized in Table 6.

Thermolysis of 9. A solution of **9** (10.7 mg, 0.011 mmol) in toluene (10 mL) placed in a Schlenk tube fitted with a condenser was heated at 110 °C under nitrogen for 17 h. The solvent was removed under reduced pressure, and the residue obtained was redissolved in the minimum volume of dichloromethane and chromatographed on TLC plates. Elution with hexane/CH₂Cl₂ (3:2 v/v) gave unreacted **9** (*R_f* = 0.24, yield = 8.3 mg, 78%) and red crystalline **10** (*R_f* = 0.50, yield = 1.2 mg, 8.7%), both identified by their IR spectrum.

Crystal Structure Determinations. Crystals were grown from dichloromethane/hexane solutions and mounted on quartz

Table 7. Crystal and Refinement Data for 3a–d and 5

	3a	3b	3c	3d	5
empirical formula	C ₁₉ H ₆ O ₁₂ Os ₃	C ₁₉ H ₆ O ₁₂ Os ₃	C ₁₅ H ₄ O ₁₂ Os ₃	C ₁₅ H ₄ O ₁₂ Os ₃	C ₁₅ H ₆ O ₁₂ Os ₃ ·CH ₂ Cl ₂
fw	996.84	1139.24	946.78	946.78	1033.72
temperature, K	223(2)	223(2)	223(2)	223(2)	223(2)
cryst syst	monoclinic	orthorhombic	triclinic	monoclinic	monoclinic
space group	<i>C2/c</i>	<i>Pbcn</i>	<i>P1</i>	<i>P2₁/n</i>	<i>P2₁/c</i>
<i>a</i> , Å	25.9456(3)	25.1390(14)	8.744(5)	7.9711(1)	9.0029(3)
<i>b</i> , Å	10.3497(1)	11.5290(6)	9.408(6)	16.7506(2)	9.9438(3)
<i>c</i> , Å	16.5559(1)	15.2961(9)	12.860(8)	14.9583(1)	25.7169(8)
α , deg	90	90	87.144(11)	90	90
β , deg	94.195(1)	90	79.807(11)	102.747(1)	92.729(1)
γ , deg	90	90	75.337(11)	90	90
volume, Å ³	4433.83(7)	4433.2(4)	1007.3(10)	1948.02(4)	2299.64(13)
<i>Z</i>	8	8	2	4	4
density (calcd), Mg/m ³	2.987	2.987	3.122	3.228	2.986
abs coeff, mm ⁻¹	17.215	17.218	18.935	19.582	16.826
<i>F</i> (000)	3552	3552	836	1672	1848
cryst size, mm ³	0.40 × 0.38 × 0.38	0.315 × 0.245 × 0.215	0.32 × 0.32 × 0.14	0.32 × 0.23 × 0.22	0.14 × 0.12 × 0.10
θ range for data collection, deg	2.12 to 29.27	2.36 to 28.52	1.61 to 30.35	1.85 to 29.31	2.20 to 30.03
no. of reflns collected	27 598	34 094	7343	14 062	18 990
no. of ind reflns	5505	5632	5064	4884	6671
	[<i>R</i> (int) = 0.0344]	[<i>R</i> (int) = 0.0628]	[<i>R</i> (int) = 0.0570]	[<i>R</i> (int) = 0.0416]	[<i>R</i> (int) = 0.0483]
completeness, % (to θ , deg)	91.0 (29.27)	99.8 (28.52)	83.4 (30.35)	91.7 (29.31)	99.3 (30.03)
max. and min. transmn	0.042 and 0.014	0.105 and 0.041	0.056 and 0.015	0.080 and 0.032	0.284 and 0.202
no. of data/restraints/params	5505/0/307	5632/5/308	5064/0/271	4884/0/275	6671/0/299
goodness-of-fit on <i>F</i> ²	1.151	1.217	1.044	1.156	1.102
final <i>R</i> indices [<i>I</i> > 2 σ (<i>I</i>)]	<i>R</i> 1 = 0.0338, w <i>R</i> 2 = 0.0805	<i>R</i> 1 = 0.0440, w <i>R</i> 2 = 0.1061	<i>R</i> 1 = 0.0685, w <i>R</i> 2 = 0.1768	<i>R</i> 1 = 0.0311, w <i>R</i> 2 = 0.0736	<i>R</i> 1 = 0.0387, w <i>R</i> 2 = 0.0847
<i>R</i> indices (all data)	<i>R</i> 1 = 0.0439, w <i>R</i> 2 = 0.0855	<i>R</i> 1 = 0.0538, w <i>R</i> 2 = 0.1087	<i>R</i> 1 = 0.0766, w <i>R</i> 2 = 0.1895	<i>R</i> 1 = 0.0401, w <i>R</i> 2 = 0.0770	<i>R</i> 1 = 0.0495, w <i>R</i> 2 = 0.0883
largest diff peak and hole, e Å ⁻³	1.162 and -1.852	1.775 and -1.893	5.139 and -3.186	1.312 and -1.948	1.884 and -2.784

Table 8. Crystal and Refinement Data for 8a, 8d, 9, and 10

	8a	8d	9	10
empirical formula	C ₁₉ H ₈ O ₁₃ Os ₃	C ₁₅ H ₆ O ₁₃ Os ₃	C ₁₅ H ₆ O ₁₂ Os ₃	C ₁₈ H ₄ O ₁₅ Os ₄ ·1/2CH ₂ Cl ₂
fw	1014.85	964.80	948.80	1263.47
temperature, K	193(2)	223(2)	223(2)	223(2)
cryst syst	monoclinic	monoclinic	orthorhombic	monoclinic
space group	<i>C2/c</i>	<i>P2₁/n</i>	<i>P2₁2₁2₁</i>	<i>C2/m</i>
<i>a</i> , Å	27.5207(11)	13.0789(3)	7.3582(3)	12.5051(6)
<i>b</i> , Å	7.4504(3)	11.6074(2)	8.9915(4)	11.7989(6)
<i>c</i> , Å	23.9268(10)	14.2418(3)	29.1969(14)	17.1181(8)
α , deg	90	90	90	90
β , deg	110.838(1)	102.461(1)	90	97.521(1)
γ , deg	90	90	90	90
volume, Å ³	4585.1(3)	2111.14(8)	1931.70(15)	2504.0(2)
<i>Z</i>	8	4	4	4
density (calcd), Mg/m ³	2.940	3.035	3.262	3.352
abs coeff, mm ⁻¹	16.653	18.075	19.748	20.412
<i>F</i> (000)	3632	1712	1680	2228
cryst size, mm ³	0.36 × 0.34 × 0.28	0.26 × 0.16 × 0.16	0.14 × 0.12 × 0.10	0.30 × 0.22 × 0.19
θ range for data collection, deg	2.81 to 31.02	2.37 to 26.37	2.37 to 29.46	2.38 to 29.42
no. of reflns collected	40289	16525	13915	17156
no. of ind reflns	7121 [<i>R</i> (int) = 0.0326]	4293 [<i>R</i> (int) = 0.0380]	4873 [<i>R</i> (int) = 0.0436]	3396 [<i>R</i> (int) = 0.0382]
completeness, % (to θ , deg)	97.1 (31.02)	99.5 (26.37)	93.5 (29.46)	93.7 (29.42)
max. and min. transmn	0.070 and 0.030	0.160 and 0.089	0.243 and 0.169	0.113 and 0.064
no. of data/restraints/params	7121/0/324	4293/0/289	4873/0/279	3396/6/206
goodness-of-fit on <i>F</i> ²	1.035	1.057	1.066	1.141
final <i>R</i> indices [<i>I</i> > 2 σ (<i>I</i>)]	<i>R</i> 1 = 0.0325, w <i>R</i> 2 = 0.0791	<i>R</i> 1 = 0.0282, w <i>R</i> 2 = 0.0640	<i>R</i> 1 = 0.0342, w <i>R</i> 2 = 0.0613	<i>R</i> 1 = 0.0250, w <i>R</i> 2 = 0.0472
<i>R</i> indices (all data)	<i>R</i> 1 = 0.0420, w <i>R</i> 2 = 0.0817	<i>R</i> 1 = 0.0364, w <i>R</i> 2 = 0.0668	<i>R</i> 1 = 0.0385, w <i>R</i> 2 = 0.0627	<i>R</i> 1 = 0.0289, w <i>R</i> 2 = 0.0482
largest diff peak and hole, e Å ⁻³	2.359 and -1.185	1.127 and -1.367	1.422 and -1.227	1.250 and -1.086
extinction coeff		0.00125(5)		

fibers. X-ray data were collected on a Bruker AXS APEX system, using Mo K α radiation, with the SMART suite of programs.¹⁴ Data were processed and corrected for Lorentz and polarization effects with SAINT¹⁵ and for absorption effects with SADABS.¹⁶ Structural solution and refinement were carried out with the SHELXTL suite of programs.¹⁷ Crystal and refinement data are summarized in Tables 7 and 8.

The structures were solved by direct methods to locate the heavy atoms, followed by difference maps for the light, non-hydrogen atoms. Organic hydrogen atoms were placed in calculated positions. All non-hydrogen atoms were generally given anisotropic displacement parameters in the final model (but see below). Metal hydrides not located in the electron density difference maps were placed in positions calculated with XHYDEX¹⁸ and refined with a fixed isotropic thermal parameter and riding on one of the osmium atoms it is

(14) SMART version 5.628; Bruker AXS Inc.: Madison, WI, 2001.

(15) SAINT+ version 6.22a; Bruker AXS Inc.: Madison, WI, 2001.

(16) Sheldrick, G. M. SADABS; 1996.

(17) SHELXTL version 5.1; Bruker AXS Inc.: Madison, WI, 1997.

(18) Orpen, G. XHYDEX: A Program for Locating Hydrides in Metal Complexes; School of Chemistry, University of Bristol: UK, 1997.

attached to. An extinction parameter was refined for **8d**, and **9** was refined as a racemic twin.

A dichloromethane solvent molecule was found in **5** and **10**; in the latter, it was disordered about a center of symmetry. The disorder was modeled with two alternative sites of equal occupancies, with appropriate restraints applied.

The coumarin ligand in **3b** exhibited disorder about a pseudomirror plane; this was modeled as two sites of equal occupancies, with appropriate restraints applied. The crystal of **3c** broke off midway through data collection, which accounted for inadequate absorption correction and hence the large residue about the heavy atoms.

Acknowledgment. This work was supported by the National University of Singapore (Research Grant No.

RP 010172), and one of us (Q.L.) thanks the University for a Research Scholarship.

Supporting Information Available: Experimental and refinement details for the crystallographic studies, tables of crystal data and structure refinement, atomic coordinates, isotropic and anisotropic thermal parameters, complete bond parameters, and hydrogen coordinates. Crystallographic data in CIF format. This material is available free of charge via the Internet at <http://pubs.acs.org>.

OM030250Z